

Experimental investigation of a novel heat pipe and porous ceramic based indirect evaporative cooler

O. E. Amer and R. Boukhanouf

*Department of Architecture and Built Environment, University of Nottingham,
University Park, Nottingham, NG7 2RD*

Abstract

The paper presents laboratory test results of an integrated heat pipe and ceramic tube based evaporative cooling prototype for air conditioning in buildings. The cooler integrates durable porous ceramic tubes as water saturated media materials and heat pipes as efficient heat transfer devices. The ceramic tubes and the heat pipes straddle across two separate air ducts to form a wet and dry channel respectively. The thermal performance of the cooler was measured at various air inlet conditions of temperature, humidity and mass flow rates. The experimental measurements show that the cooling system can provide sufficient cooling as high as 1220 W/m^2 of the wet media exposed surface area and depressing ambient temperature to 12°C . Equally, it was measured that the wet bulb effectiveness of the cooler can reach 86%.

Keywords: indirect evaporative cooling, heat pipe, porous ceramic tube

1. Introduction

Many people spent longer time indoors which consequently contributes, with other factors, towards higher electricity consumption in building. The advancement of HVAC technologies and mass productions participated in the vast expansion of the HVAC market. As a result, building energy demand continuously is rocketing up. For example, in the MEAN region 70% of energy consumption in buildings is accounted for air conditioning and cooling systems which approximately represent 30% of their total prime energy demand. Hence, improving the efficiency of cooling technologies and reducing electricity consumption are vital matters. The evaporative cooling method appears as a peer to other traditional and market dominant coolers i.e. the vapour compression cooling systems. As most evaporative coolers only employ a small fan and water pump, therefore, their power consumption is low. Also, the usage of water as a refrigerant, instead of hazardous refrigerants e.g. R-22, classifies it as environmentally friendly system. However, the performance dependency on the ambient air conditions and relatively high water consumption are the main drawbacks of the evaporative coolers [1].

In the literature, heat pipes have been applied effectively in several cooling applications such as electronics cooling, power plants, thermal energy storage, solar water heating and HVAC [2]. In the literature, many research studies have been found of heat pipes applications in building cooling include HVAC systems [3] and [4], heat recovery systems [5] and [6] and air ventilation [7] and [8]. Yet limited research work has been found on heat pipe based indirect evaporative coolers for building air cooling [9]. [10], [11] proposed a building integrated heat pipes system cooling system. This configuration consists of two adjacent channels; one for indoor-air and another for outdoor-air where heat pipes are fitted horizontally across both passages. The heat pipe evaporator is finned to increase convective heat transfer rate, while heat pipe condenser is embedded in a ceramic water container exposed to ambient air. Additionally, similar work carried out by [12] and [13] used the same configuration proposed by [10] except from using of water sprayers to cool down the heat pipe condensers which are wrapped with a

* **Corresponding author:** Omar E. Amer, Email: ezxoea@nottingham.ac.uk.

thin layer of an absorbent material rather than using ceramic containers, the findings, from [12], shown an effectiveness of 70%.

As the above review shown, studies related to the application of heat pipe and wet ceramic tubes for building cooling have been relatively scanty, and that there is no study focusing on employing both heat pipes and porous ceramic material together of a self-contained and stand-alone IEC system. Accordingly, the present study aims to experimentally investigate the thermal performance of a stand-alone heat pipe and porous ceramic IEC system under several climate conditions; and study the effects of the ambient temperature and humidity on the performance.

2. System construction and experimental set-up

The system consists of outside casing, tubular heat pipes, cylindrical porous ceramic tubes, a damper, and a fan. The casing is made from 5mm thick transparent Perspex sheets which are firmly fitted to form two adjacent ducts with a non-permeable and adiabatic plate, the heat pipes are vertically placed across the common wall, as illustrated in Fig 1. The heat pipes made from copper with wire mesh wick structure and water as a working fluid. Each heat pipe is 30 cm in length and 18 mm of outer diameter, and the cylindrical ceramic tube is 150 mm in length and 28 mm of the outer diameter.

The working principle of this cooler principally is based on the modified M-cycle of IEC system in which fraction of the cooled supply air is diverted to the wet channel to become the working air. This configuration allows extra amount of energy to transport from both the dry- and wet-air passage instead of using the hot ambient air as working fluid. A cross-sectional view of the rig presents the working principles of the system is shown in Fig 1. The inlet air enters the dry air channel (state 3) and passes through the finned heat pipe evaporators (HPE) (state 3) where the air is cooled down by transporting heat via the finned heat pipes to the wet channel, till just before the exit of the dry channel where part of the cooled inlet air is fractioned and diverted into the wet channel (state 6), while, the remaining part of the air stream is supplied to the conditioned room (state 5). In the upper duct, the heat pipe condensers (HPCs) are embedded in the ceramic tubes and filled up with water which is supplied at 23 °C via overhead tank, the water flow down and fill up the 3 mm cavity between the outer surface of the HPC and ceramic tubes providing even and complete covering of the condenser. Therefore, the cooled working air flows in counter-current pattern, over the wetted porous ceramic tubes, as the water starts to siphon through the micro pores of the ceramic forming a tiny water film over the ceramic surface, causing a drop in the water temperature and increase of the latent heat of the working air, this process attain constant remove of the heat which would accumulate in the water due to heat transport to the condenser surface. As result, the working air is rejected to the surroundings as hot and humid air (state 7).

The experimental test-rig for this study consists of the environmental chamber; the apparatus; a blower; hoses; and measuring devices such as Thermocouples, Data logger, Humidity meters and anemometer. All these component and devices were installed and connected together to form one whole test-rig as presented in Fig 1 . The experimental test-rig assembled at Marmont laboratory of the University of Nottingham, the cooling system is connected to an environmental chamber via a flexible duct. The chamber is equipped by a control panel for setting and controlling the temperature and humidity. The hot inlet air is drawing from the chamber (point 1) through the duct (point 2) by a centrifugal fan (point 3) and flown through the dry air channel (point 4) where its heat is transferred via the heat pipes to the wet channel. At just the exit of the dry channel, part of the cooled supply air leaves towards the conditioned room (point 5) and the other part is diverted to the upper channel (point 6) for heat dissipation process form the wetted porous tubes, and then is rejected to the surrounding as humid working air (point 7).

The fan speed is controlled through a fan speed controller; where air flow rates ranged from 75-150 m³/h measured using a portable hotwire anemometer (Testo 405-V1) has range of 0-10 m/s with $\pm 5\%$ accuracy. Also, Two humidity and temperature meters (RS-232) are located at inlet of dry channel and exit of the wet channel, their working range is 20-60 °C, 10-95% RH and accuracy of $\pm 0.5\text{ }^{\circ}\text{C}$ and $\pm 1\%$ RH. In terms of sensors, 8 (K-type) thermocouples, working range from -50 to +250°C and accuracy of $\pm 0.4\%$, were installed in several points to measure temperatures on air flow passages and feed water simultaneously, as shown in Fig 1. All the thermocouples are connected to data acquisition device i.e. data taker (DT500 series 2) connected to a computer which runs a program called DeLogger-4 for instant monitoring and data logging of any sent experimental readings by data taker which set to be every 20 seconds. While, the humidity values and added water amounts are manually recorded every 3 minutes.

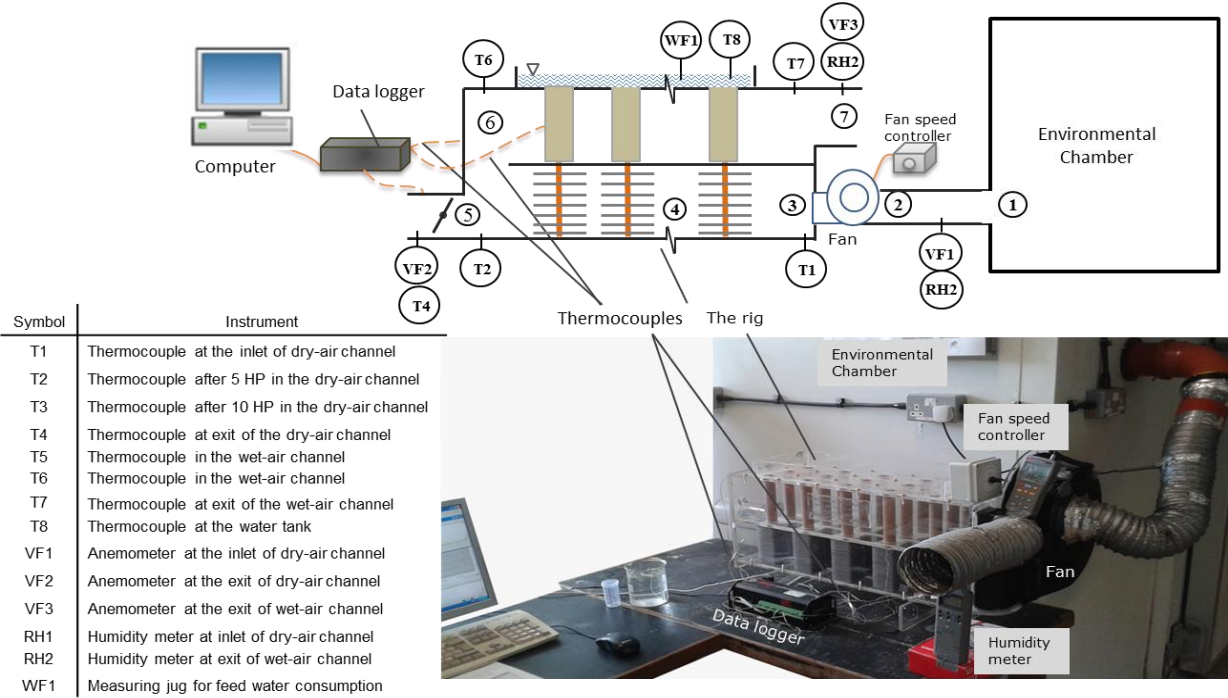


Fig 1 Schematic of the rig and the experimental setup

3. Test conditions

Several test conditions were conducted in order to characterise the thermal performance over a range of climatic conditions which adequately represent the climate of hot and dry areas such as the MENA region. For the experimental study, Fig 2 illustrates the test conditions plan of the conducted experiments, each test lasted from 30 to 45 min.

4. Mathematical model

A mathematical model was developed to investigate the thermal performance and study the design parameters of this system. In the model, the domain of interest is divided into “n” elements a cross both the dry- and wet-air channel as shown in Fig 3. By applying energy and mass conservation laws, a set of differential governing equations are formulated as follows [14].

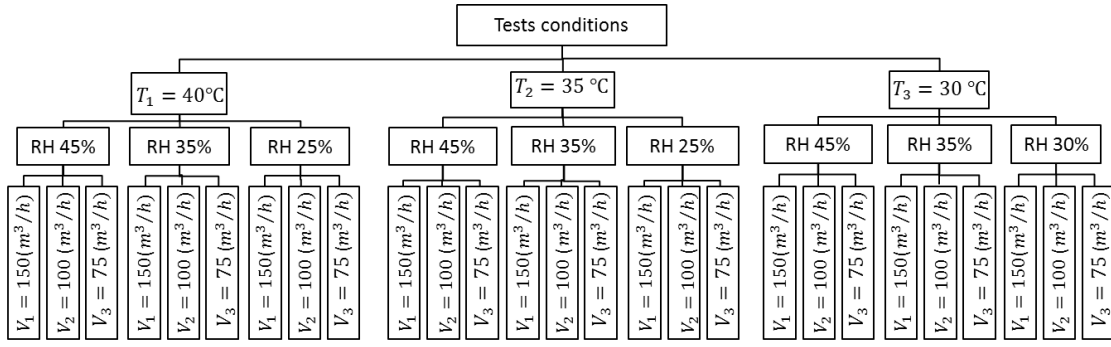


Fig 2 Test conditions plan

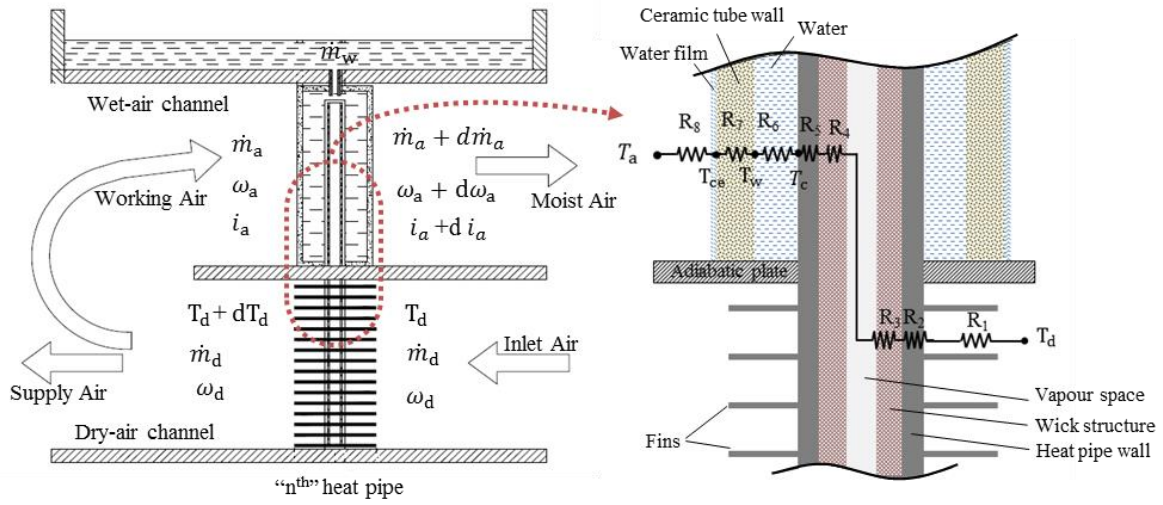


Fig 3 Schematic of heat pipe and ceramic tube module

Energy balance of supply air in the dry channel side gives:

$$\dot{m}_d c_{P,d} dT_d = - U_d A (T_d - T_w) \quad (1)$$

$$Q_1 = \dot{m}_d c_{P,d} dT_d \quad (2)$$

where, Q_1 is maximum heat transferred by a heat pipe which is the minimum value of heat transfer limitations of the heat pipe, W [15]; \dot{m}_d is air flow rate in the dry-air channel, kg/s; T_d is temperature in the dry channel, °C; T_w is water temperature, °C; U_d is overall heat transfer coefficient between both channels, W/m^2K , which is expressed as

$$U_d = \frac{1}{\sum R} = \frac{1}{R_{1,conv} + R_{2,cond} + R_{3,cond} + R_{4,cond} + R_{5,cond} + R_{6,water}} \quad (3)$$

$$U_d = \left(\frac{1}{h_d \eta_o A_1} + \frac{\ln(r_3/r_2)}{2\pi l_e \lambda_e} + \frac{\ln(r_2/r_1)}{2\pi l_e \lambda_{wk}} + \frac{\ln(r_2/r_1)}{2\pi l_c \lambda_{wk}} + \frac{\ln(r_3/r_2)}{2\pi l_c \lambda_c} + \frac{\ln(r_6/r_3)}{2\pi l_c \lambda_{wt}} \right)^{-1} \quad [4]$$

where, h_d is convective heat transfer coefficient in the dry-air passage, W/m^2K ; A_1 is the total area of heat transfer of the finned heat pipe, m^2 ; η_o is the overall surface efficiency of the fin; l_e is evaporator length, m; l_c is condenser length, m; λ_e is evaporator thermal conductivity, W/mK ; λ_c is condenser thermal conductivity, W/mK ; λ_{wt} is evaporator thermal conductivity,

$W/m K$; r_1 is vapour space radius of heat pipe, m; r_2 is inner radius of heat pipe evaporator, m; r_3 is outer radius of heat pipe evaporator, m; r_6 is inner radius of the porous ceramic tube, m.

Mass balance of the moist air in the moist-air channel yields:

$$\dot{m}_a d\omega_a = h_m dA(\omega'_{wf} - \omega_a) \quad [5]$$

Energy balance of the moist air in the wet air channel side gives:

$$\dot{m}_a di_a = h_a dA(T_{wf} - T_a) + h_m dA(\omega'_{wf} - \omega_a) i_{v,ce} \quad [6]$$

Energy balance of the water film gives:

$$\dot{m}_{wf} di_{wf} = U_o A(T_d - T_w) - h_m A(\omega'_{wf} - \omega_a)(i_{v,w} - i_{l,w}) - h_a A(T_{wf} - T_a) \quad [7]$$

where, \dot{m}_a is the moist air mass flow rate in the wet-air channel, kg/s ; i_a is the enthalpy of the moist air, J/K ; h_a is the convective heat transfer coefficient in the wet-air channel, W/m^2K ; A is the area of heat transfer, m^2 ; T_{wf} is the water film temperature, $^{\circ}C$; T_a is the moist air temperature, $^{\circ}C$; h_m is the mass transfer coefficient, m/s ; ω'_{wf} is saturated air moisture content at water film temperature, kg_{water}/kg_{air} ; ω_a is moist air moisture content, kg_{water}/kg_{air} ; $i_{v,ce}$ is the enthalpy of water vapour at temperature of ceramic surface, J/K ; c_{pa} is moist air specific heat, $J/kg K$; \dot{m}_{wf} is water film mass flow rate, kg/s ; T_{ce} is the ceramic surface temperature, $^{\circ}C$.

5. Results and discussion

The performance along with the main characteristics of the evaporative cooler conditions of 40 $^{\circ}C$ of inlet air temperature, 25% and 45% relative humidity are summarised in Table 1. For such inlet conditions and with inlet flowrates from 75 to 150 (m^3/h), the air temperature is cooled down to ranges of 28.30-32.3 $^{\circ}C$, with a corresponding cooling capacity of 727.83-1219 (W/m^2) respectively. The water consumption ranged 150-450 (ml/h) depending on the inlet air conditions. As it can be seen from the table, the cooler was able to drop the temperature of the ambient air (40 $^{\circ}C$, 25% RH and 75 m^3/h) by almost 12.0 $^{\circ}C$ with WB and DP effectiveness of 71.3% and 48.7%, respectively.

Table 1 System performance at inlet conditions of 40 $^{\circ}C$, 25% and 45% RH, and 50% flowrate ratio of supply-to-inlet air

Parameters	Values			Values		
Inlet air temperature and relative humidity	40 $^{\circ}C$, 25%			40 $^{\circ}C$, 45%		
Volumetric flow rate of inlet air (m^3/h)	150.0	105.00	75.00	150.0	105.00	75.0
Volumetric flowrate of supply air (m^3/h)	74.9	52.55	37.70	74.9	52.55	37.7
Supply air temperature ($^{\circ}C$)	30.25	28.80	28.30	32.30	31.15	30.65
Supply air relative humidity (%)	43.00	46.00	48.00	68.00	73.00	75.00
Temperature reduction of inlet air ($^{\circ}C$)	9.75	11.2	11.7	7.7	8.85	9.35
Wet-bulb effectiveness (%)	59.5	68.3	71.3	70.6	81.20	85.80
Dew-point effectiveness (%)	41.00	47.10	48.70	54.2	62.30	65.80
Cooling capacity (W/m^2)	1219	982.8	727.83	974.25	786.00	589.3

The effect of inlet air temperature and humidity on the effectiveness and the cooling capacity

Fig 4 presents the WB effectiveness and cooling capacity profiles versus inlet air temperatures for a constant inlet air flow rate of $105 \text{ (m}^3/\text{h)}$ and inlet humidity of 45% and 35%. It was found that the effectiveness of the system improved gradually as the inlet air temperature increased for different values of the inlet relative humidity. For the inlet air conditions of $35 \text{ }^\circ\text{C}$ and 45% RH, the WB effectiveness was 79.6%. While, at higher inlet temperature of $40 \text{ }^\circ\text{C}$ the WB effectiveness reached 86%. This obviously indicates to one of the advantages of the evaporative coolers over other conventional vapour-compressed cooling systems, that, the performance of the system increases as the ambient temperature rises. Additionally, the effect of varying inlet humidity on the effectiveness can be observed, that is, the best values of effectiveness were associated with higher values of inlet humidity at constant air temperature.

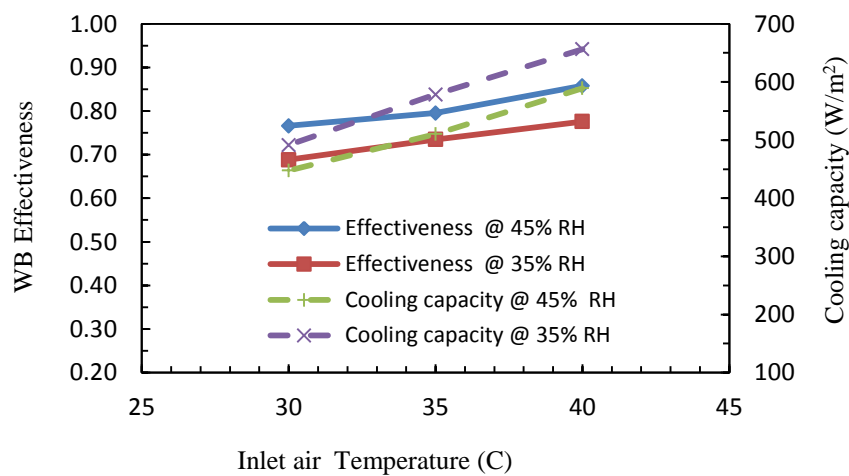


Fig 4 Effectiveness and cooling capacity versus inlet air temperature at $75 \text{ (m}^3/\text{h)}$ flow rate

Regarding the cooling capacity, as it can be seen from

Fig 4, the increase of the inlet air temperature affected positively on the cooling capacity. This possibly because of the increase of temperature reduction of the supply air as the inlet air temperature increases. Furthermore, the best values of cooling capacities were achieved at the lower values of relative humidity at constant inlet temperature. For example, at given conditions of 40°C , 35% RH, the best cooling capacity of the system was about $656 \text{ (W/m}^2)$. Moreover, it is apparent from the

Fig 4 that the high cooling capacities were associated with low values of inlet air humidity, thus, their relation is inversely proportional.

Further evaluation of the cooler performance at various ambient conditions was conducted. Fig 5 compares the effect of changing inlet air flow rate on the effectiveness and the cooling capacity. From the figure below, an inverse correlation exists between the effectiveness and inlet air flow rate. For example, at inlet air flow rate of $75 \text{ (m}^3/\text{h)}$ the WB effectiveness was about 86%, as the air flow rate is doubled the effectiveness declined by 17.70%. By comparing, the cooling capacity is directly proportional with the inlet air flow rate. The cooling capacity rose considerably as the inlet flow rate increased. It increased from 589.3 to $974.3 \text{ (W/m}^2)$ as the flow rate rose from 75 to $150 \text{ (m}^3/\text{h)}$. This possibly because of the large flow rates passing through the system at high speed e.g. ($150\text{m}^3/\text{h}$) which would promote the values of cooling capacity, due to a direct proportional relation between the cooling capacity and flow rate. As seen from the slope of curves, the inlet air flow rate tends to have a greater effect on the cooling capacity than it would on the effectiveness.

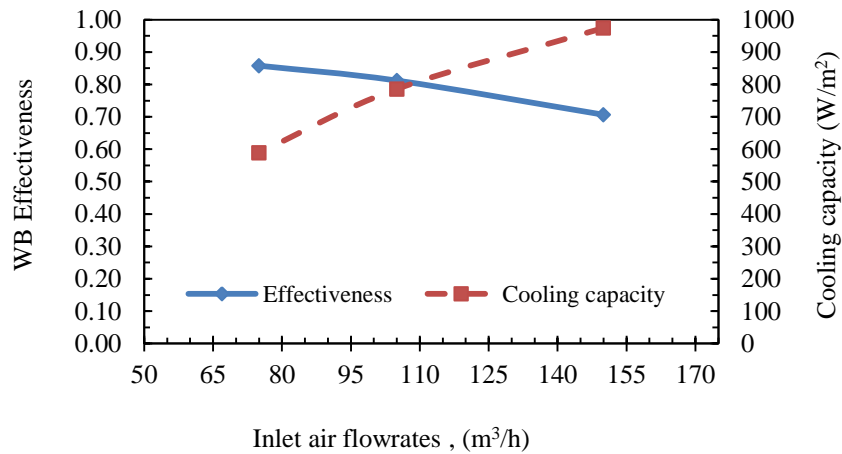


Fig 5 Effectiveness and cooling capacity versus flow rates at inlet conditions 40 C and 45% RH

6. Result validation

To validate the computer model, the experimental results were used for model verification by comparing the findings from both. Fig 6 illustrates a comparison between temperature profiles of inlet air temperature (T_d) and moist air temperature (T_a) of both the experiment and the numerical results. As it can be seen, a good agreement between the predicted result and the experimental findings was found, with maximum deviation about $\pm 1\%$ of the inlet air temperature.

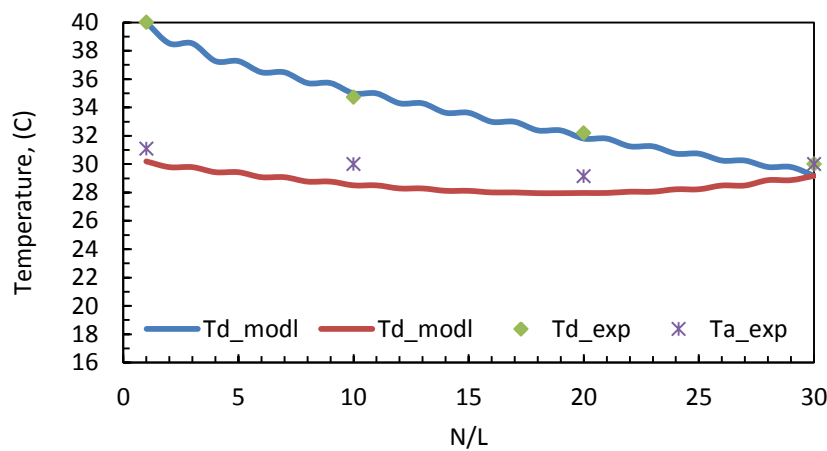


Fig 6 Temperature profiles along the cooler

7. Conclusions

An experimental investigation was conducted in order to evaluate the performance and determine the effect of various operation conditions on the new indirect evaporative cooler. The cooler was able to drop to the inlet air temperature by 12°C, and the WB effectiveness of 86% was achievable. Also, the cooling capacity of the system reached of 1220 (W/m^2) associated with 60% WB effectiveness. In addition, from simulation results, a good agreement found between the experimental and numerical results. Further design adjustments and amendments are recommended to improve the performance. Such as, increase the surface area of the cooling system either by increasing number of the heat pipe and ceramic tube modules or increase the diameter of the tubes, and reduce the width of the upper channel which would increase heat

transfer coefficient by ensuring existence of the turbulence flow which would make the working air contact as much as possible of the outer surfaces of the ceramic tubes.

References

1. Amer, O., R. Boukhanouf, and H. Ibrahim, A Review of Evaporative Cooling Technologies. in *International Journal of Environmental Science and Development* 2015. p. 111-117.
2. Shabgard, H., et al., Heat pipe heat exchangers and heat sinks: Opportunities, challenges, applications, analysis, and state of the art. *International Journal of Heat and Mass Transfer*. 2015. **89**: p. 138-158.
3. Abd El-Baky, M.A. and M.M. Mohamed, Heat pipe heat exchanger for heat recovery in air conditioning. *Applied Thermal Engineering*, 2007. **27**(4): p. 795-801.
4. Calautit, J.K., et al., Comparison between evaporative cooling and a heat pipe assisted thermal loop for a commercial wind tower in hot and dry climatic conditions. *Applied Energy*. 2013. **101**(0): p. 740-755.
5. Herrero Martín, R., F.J. Rey Martínez, and E. Velasco Gómez, Thermal comfort analysis of a low temperature waste energy recovery system: SIECHP. *Energy and Buildings*. 2008. **40**(4): p. 561-572.
6. Mathur, G. Enhancing performance of an air conditioning system with a two-phase heat recovery loop retrofit. in Energy Conversion Engineering Conference, 1996. *IECEC 96., Proceedings of the 31st Intersociety*. 1996. IEEE.
7. Zhang, L. and W.L. Lee, Evaluating the use heat pipe for dedicated ventilation of office buildings in Hong Kong. *Energy Conversion and Management*, 2011. **52**(4): p. 1983-1989.
8. Chaudhry, H.N. and B.R. Hughes, Climate responsive behaviour of heat pipe technology for enhanced passive airside cooling. *Applied Energy*. 2014. **136**: p. 32-42.
9. Boukhanouf, R., et al., Experimental and Numerical Study of a Heat Pipe based Indirect Porous Ceramic Evaporative Cooler, in *International Journal of Environmental Science and Development* 2015. p. 104.
10. Riffat, S.B. and J. Zhu, Mathematical model of indirect evaporative cooler using porous ceramic and heat pipe. *Applied Thermal Engineering*. 2004. **24**(4): p. 457-470.
11. Riffat, S. and J. Zhu, Experimental investigation of an indirect evaporative cooler consisting of a heat pipe embedded in porous ceramic. *J Res*, 2003. **1**: p. 46-52.
12. Huang, X., et al., Theory and applications of evaporative cooling air conditioning. *China Architecture & Building Press*, Beijing, 2010.
13. X.J. Wang, X.H., J.M. Wu, Analysis of a novel indirect evaporative cooler with heat pipe heat exchanger. *Fluid Machinery*, 2004. **32**(2): p. 72-74.
14. Halasz, B., A general mathematical model of evaporative cooling devices. *Revue Générale de Thermique*, 1998. **37**(4): p. 245-255.
15. Chi, S., *Heat Pipe Theory and Practice: A sourcebook*. Washington: Hemisphere Pub. Corp, 1976.